P1.2 **Calculation of turbulence intensity based on spectrum width data of a Doppler LIDAR**

C.C. Wong
The University of Hong Kong

P.W. Chan *
Hong Kong Observatory, Hong Kong, China

K. Akaeda and H. Mizuno
Japan Meteorological Agency

1. INTRODUCTION

In addition to low-level windshear (below 1600 feet), low-level turbulence could also adversely affect arriving/departing aircraft at the airport. Turbulent airflow may occur in clear-air/non-rainy weather conditions, e.g. terrain effect at the Hong Kong International Airport (HKIA) or building's disruptions at Haneda Airport (Tokyo International Airport) in Japan. Such airflow disturbances could be monitored by LIght Detection And Ranging (LIDAR) systems.

In aviation meteorology, turbulence intensity is expressed in terms of the cube root of eddy dissipation rate (EDR). Chan and Kwong (2008) calculated EDR using the structure function approach based on the Doppler velocity measurements from the LIDAR systems at HKIA. The EDR values so calculated appear to successfully capture some cases of turbulent flow in Hong Kong. However, the computational efficiency is rather low for this approach so that it may only be suitable for post analysis of low-level turbulence events instead of real-time implementation. An alternative method for LIDAR-based turbulence intensity calculation is based on the spectrum width data. Unfortunately, the Hong Kong systems have only limited digitization power for the Doppler spectrum (64 bits Fast Fourier Transform, FFT) and thus the spectrum width data are not of sufficient quality to estimate EDR.

Equipped with better digitization power (256-bit FFT), the LIDAR system at Haneda Airport, Japan is in a better position to produce spectrum width data of high quality for the computation of EDR. This paper aims at studying the calculation of turbulence intensity using the spectrum-width approach and comparing the results with that determined from the structure function approach. Some examples of spectrum width-based EDR maps would also be presented.

2. CALCULATION OF EDR FROM LIDAR'S SPECTRUM WIDTH

Technical details of the computation of EDR based on spectrum width data of a LIDAR could be found in Smalikho et al. (2004, 2005). Only a summary of the major steps is given here. The measured spectrum width (denoted by $\hat{\sigma}_{SW}$) is first corrected for spectral broadening due to probing pulse, window effect and the variance of the intermediate frequency, which are given by the three terms on the right hand side of the following equation:

$$\sigma_0^2 = (\lambda/2)^2[\sigma_{M_f}^2 + (8\pi^2\sigma_W^2)^{-1} + \sigma_\delta^2]. \qquad (1)$$

Further correction is made due to windshear effect:

$$\sigma_S^2 = (2\pi)^{-1}(\mu\Delta z)^2 \qquad (2)$$

(where μ is the windshear and Δz is the range gate size, which is about 102 m) and the error in spectrum width estimation arising from the spectrum fluctuations <*E*> (which is difficult to estimate and taken to be zero here). The corrected spectrum width is then given by:

$$\begin{aligned}\hat{\sigma}_t^2 &= \left\langle \hat{\sigma}_{SW}^2 \right\rangle_E - \sigma_0^2 - \sigma_S^2 - \langle E \rangle \\ &= \left\langle \hat{\sigma}_{SW}^2 \right\rangle_E - \sigma_0^2 - \sigma_S^2, \end{aligned} \qquad (3)$$

where $<>_E$ is ensemble average.

In the calculation of velocity fluctuation, the turbulent wind component is first computed, which is the measured Doppler velocity minus the mean velocity:

$$\hat{v}_D'(R,\theta,k) = \hat{v}_D(R,\theta,k) - \bar{v}_D(R,\theta,k), \qquad (4)$$

where *R* is the range, *θ* the azimuth angle and *k* the time index. The mean velocity is obtained by averaging the Doppler velocities within the subsector of LIDAR scanning under consideration (which is taken to be 10 range gates and 14 azimuth angles as in Chan and Kwong (2008)). Fluctuation of the measured Doppler velocity is then given by:

$$\hat{\sigma}_{\hat{V}_D}^2 = \left\langle (V_D')^2 \right\rangle, \qquad (5)$$

where <> is the average over the LIDAR measurement sector under consideration. The wind fluctuation should be corrected for the uncertainty in the Doppler velocity measurement. An estimate of this uncertainty is expressed in terms of a covariance function:

$$\begin{aligned}&\hat{C}(n\Delta z) \\ &= N^{-1}\sum_{l,k}\hat{v}_D'(l\Delta z,k)\times\hat{v}_D'((l+n)\Delta z,k)\end{aligned} \qquad (6)$$

where the summation is made over all the possible locations within the subsector with index *l* and the time *k*, with N being the total number of items in the

* *Corresponding author address:* P.W. Chan, Hong Kong Observatory, 134A Nathan Road, Hong Kong email: pwchan@hko.gov.hk

summation. The error term *e* is then given by:

$$e = \hat{C}(0) - 2\hat{C}(\Delta z) + \hat{C}(2\Delta z) \quad (7)$$

and the variance arising from uncertainty in the Doppler velocity measurement is given by:

$$\hat{\sigma}_e^2 = \left\langle e^2 \right\rangle . \quad (8)$$

With the above, the total wind fluctuation (based on the corrected fluctuation of the measured Doppler velocity over a subsector and the corrected spectral broadening at the pulse level) is calculated as follow:

$$\hat{\sigma}_V^2 = \hat{\sigma}_{\hat{V}_D}^2 - \hat{\sigma}_e^2 + \hat{\sigma}_t^2 . \quad (9)$$

It turns out that the ratio of the quantities on the left hand side of Equations (3) and (9) is given by an analytical expression:

$$\sigma_t^2 / \sigma_V^2 = F_W (L_V / \Delta z) , \quad (10)$$

where L_v is related to the outer scale of turbulence. F_w is given by the following expression:

$$F_W(L_V / \Delta z) = (1.972)^{2/3} C_K^{-1} L_V^{-2/3} G_W (\Delta z, L_V) \quad (11)$$

In which $C_K \approx 2$ is the Kolmogorov constant and G_w equals to:

$$G_W (\Delta z, L_V) = 0.2485 C_K \Delta z^{2/3} \int_0^\infty \frac{d\xi \{1 - \exp[-\xi^2 /(2\pi)]\}}{[\xi^2 + (0.746 \Delta z / L_V)^2]^{5/6}} . \quad (12)$$

Equation (10) is solved for L_v only by iteration instead of solving for both the velocity fluctuation and the turbulence scale as in the structure function approach. Thus, the spectrum-width approach is computationally more efficient and more suitable for real-time implementation. With L_v determined, EDR (ε) is calculated by using Equation (9) at the same time:

$$\varepsilon = \frac{1.972}{C_K^{3/2}} \frac{\sigma_V^3}{L_V} . \quad (13)$$

3. COMPARISON OF EDR CALCULATED BY DIFFERENT METHODS

The EDR values calculated by the two methods, viz. spectrum width approach and structure function approach, are compared using the LIDAR data from Haneda Airport. Data of five days have been considered, namely, turbulent airflow on 31 May 2007 and 5-6 September 2007, as well as the light wind days on 10 and 12 March 2008. For each day, LIDAR data of a few hours are included in the study. To achieve a fair comparison, both methods consider similar subsectors in the LIDAR scanning region, and use the same period (15 minutes) in the sampling of turbulent eddies.

The comparison result is shown in Figure 1. Both datasets are well correlated, covering light (~0.1 $m^{2/3}s^{-1}$) to severe (~0.5 $m^{2/3}s^{-1}$) turbulence. For the best-fit straight line, the slope is close to 1 and the y-intercept is close to 0. The root-mean-square difference between the two sets of data is about 0.098 $m^{2/3}s^{-1}$.

At the limit of large L_v, viz. $\Delta z \ll L_V$, it is shown in Smalikho (2004) that EDR could be given by an analytical expression:

$$\varepsilon = \frac{1}{\Delta z} \left[\frac{\sigma_t^2}{0.247 C_K} \right]^{3/2} , \text{ or } \varepsilon^{1/3} = 0.3065 \sigma_t . \quad (14)$$

For the dataset under consideration, the relation between the cube root of EDR and σ_t is shown in Figure 2. It could be seen that the two quantities could be fitted quite well by a linear equation, and the proportionality factor is close to the analytical value given in Equation (14).

4. EXAMPLES OF EDR MAP

At Haneda Airport, there may be turbulent airflow downwind of the hangars over a runway in easterly wind condition. To demonstrate the EDR maps obtained by spectrum width approach in the present study, two cases of hangar-induced turbulent flow are considered, namely, when Tokyo was under the influence of a frontal low on 31 May 2007, and the proximity of Typhoon Fitow on 5-6 September 2007. The synoptic pressure patterns at the surface in these two cases are shown in Figure 3.

The EDR maps in the two events are shown in Figures 4(a) and 5(a). The more turbulent flow area downstream of the hangars is highlighted in red in both figures with $EDR^{1/3}$ reaching about 0.5 $m^{2/3}s^{-1}$, i.e. severe turbulence. As discussed in Section 3, the $EDR^{1/3}$ values seem to have good correlation with the corrected spectrum width σ_t, the distribution of which is given in Figures 4(b) and 5(b).

5. CONCLUSIONS

The possibility of calculating EDR by using spectrum width data of a LIDAR with good digitization power for the spectral data (256-bit FFT) is demonstrated in this study based on the LIDAR system at Haneda Airport. The EDR values computed from this approach are found to have good correlation with those determined from structure function approach and the corrected spectrum width values. The spectrum width approach only requires the determination of one parameter, namely, the outer scale of turbulence, by iteration method in an implicit equation, instead of determining two parameters in the structure function approach. As such, this approach is computationally more efficient and thus more suitable for real-time implementation. For two cases of turbulent airflow associated with hangars at Haneda Airport, the turbulent wind areas are captured successfully in the EDR maps. Following the upgrade of the signal processors of the LIDARs at HKIA, a larger dataset would be used to evaluate the spectrum width approach of EDR computation.

References

Chan, P.W., and K.M. Kwong, 2008: Performance of LIDAR-based turbulence detection algorithm. *13th Conference on Aviation, Range and Aerospace Meteorology*, New Orleans, Louisiana, USA, 20-24 January 2008.

Frehlich, R.G. et al., 2006: Measurements of boundary layer profiles in an urban environment. *J. Appl. Meteor. and Climat.*, **45**, 821-837.

Smalikho, I., F. Köpp, and S.Rahm, 2004: Measurement of atmospheric turbulence by 2-μm Doppler Lidar. Report No. 200, Deutsches Zentrum für Luft- und Raumfahrt.

Smalikho, I., F. Köpp, and S.Rahm, 2005: Measurement of atmospheric turbulence by 2-μm Doppler Lidar. *J. Atmos. Oceanic Technol.*, **22**, 1733-1747.

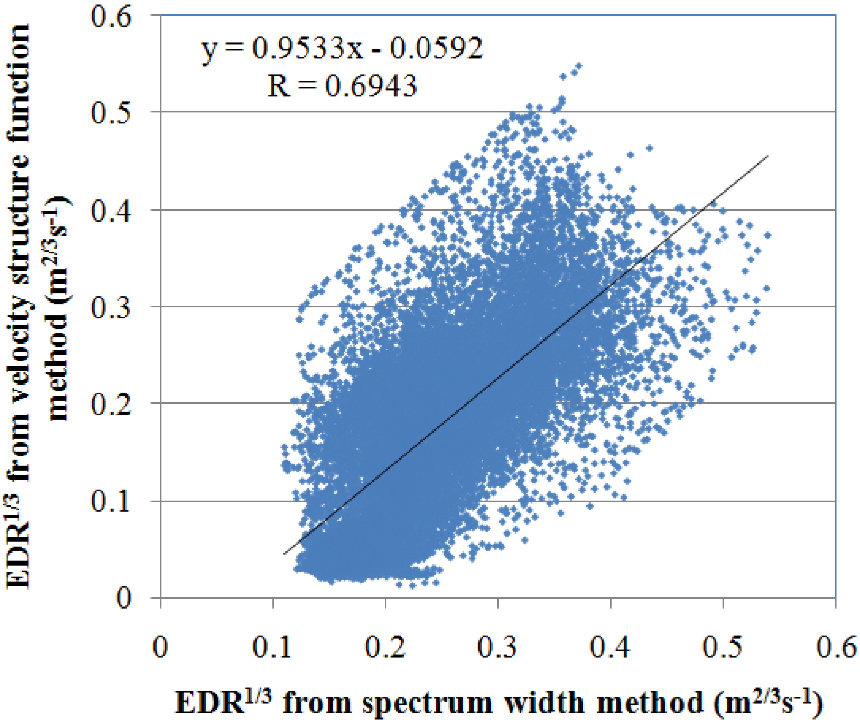

Figure 1 Comparison of EDR calculated from the two methods.

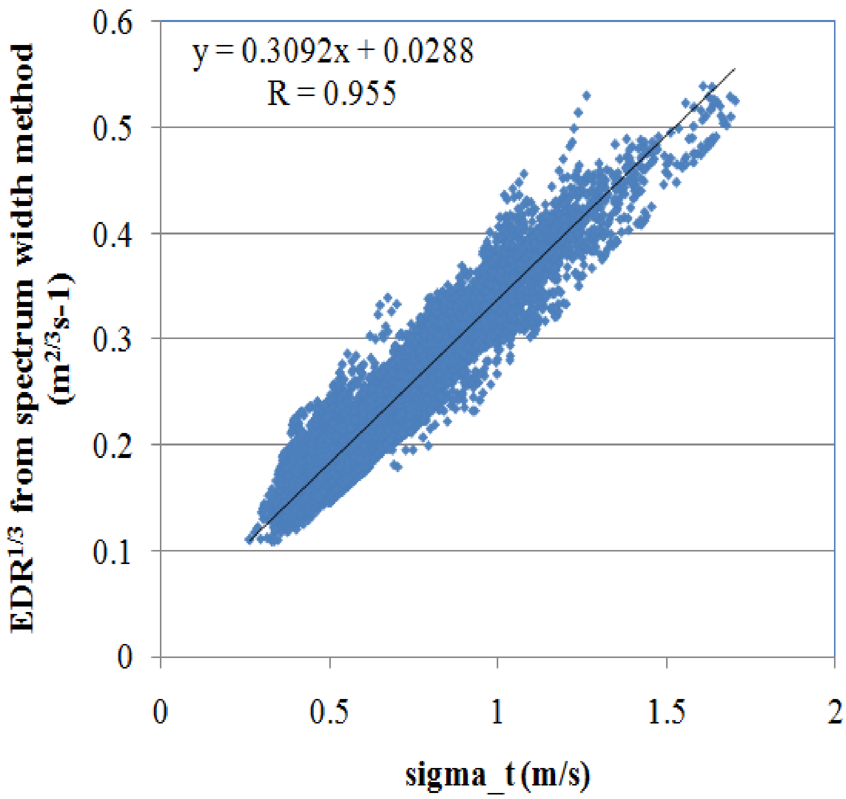

Figure 2 Comparison between EDR and the corrected spectrum width.

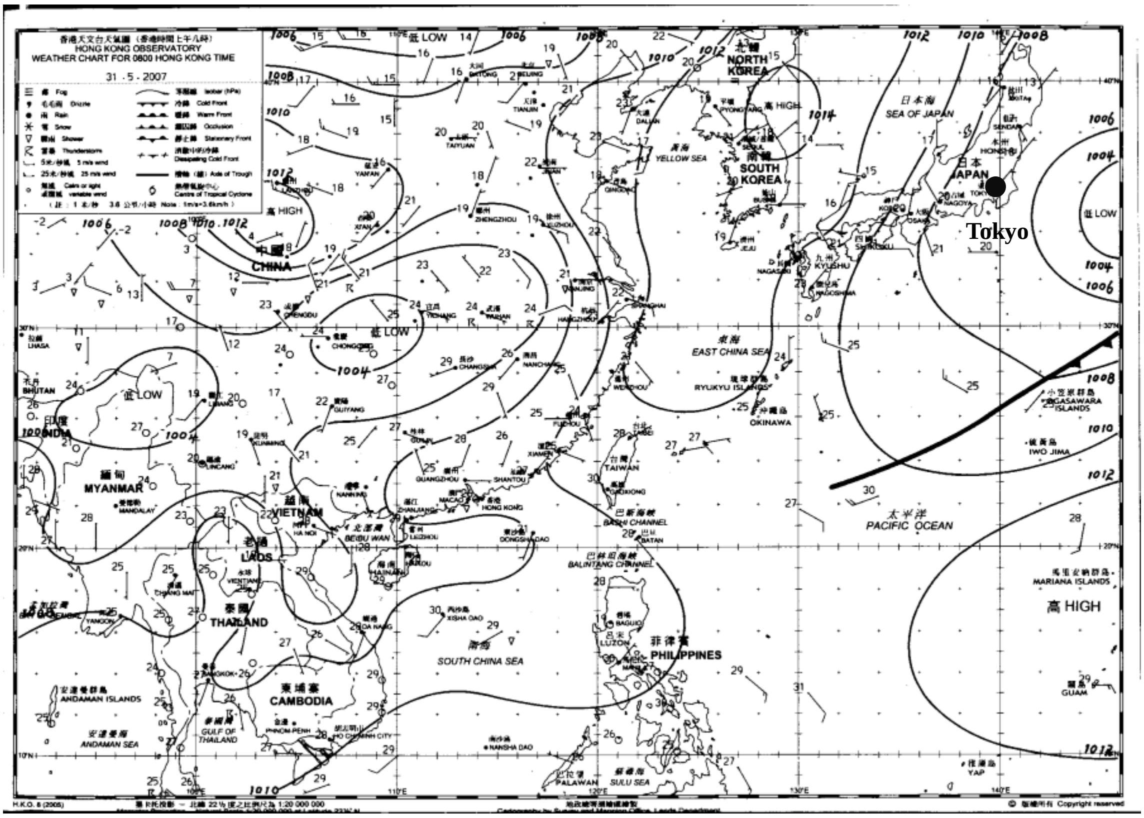

(a)   00 UTC, 31 May 2007

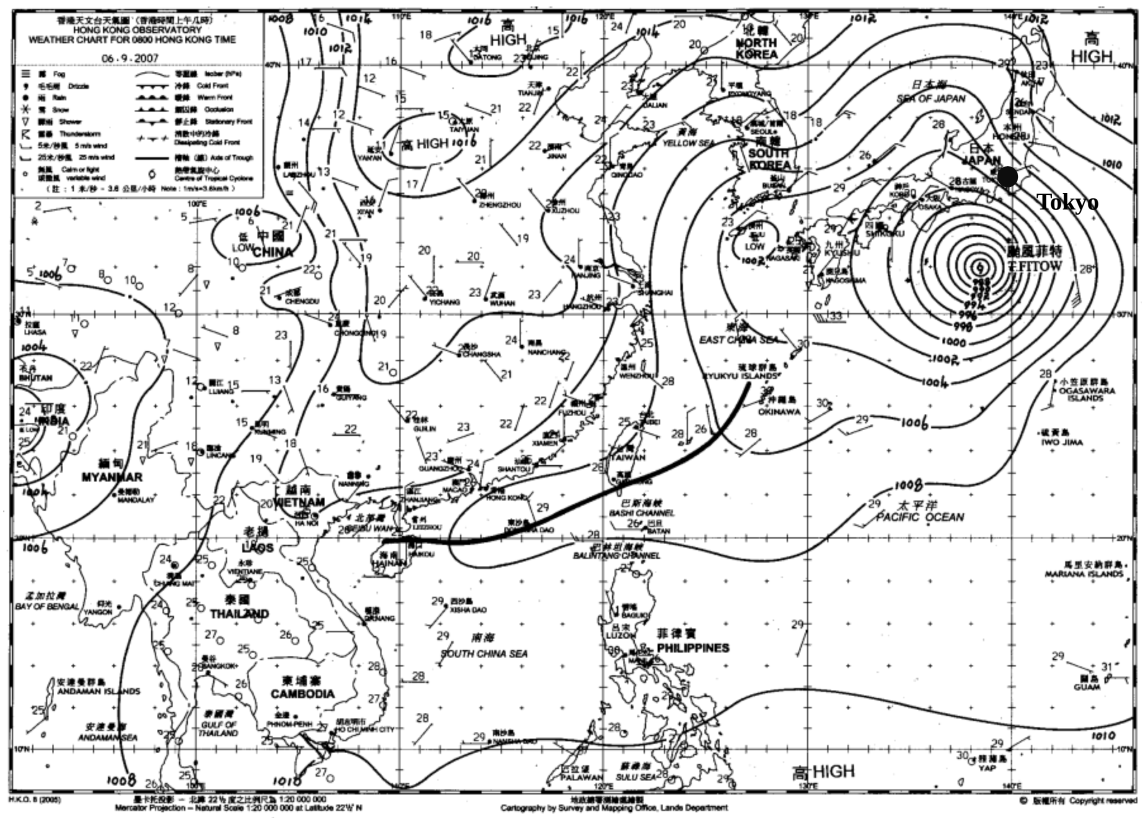

(b)   00 UTC, 6 September 2007

Figure 3   Surface isobaric charts for the cases studied in the present paper.

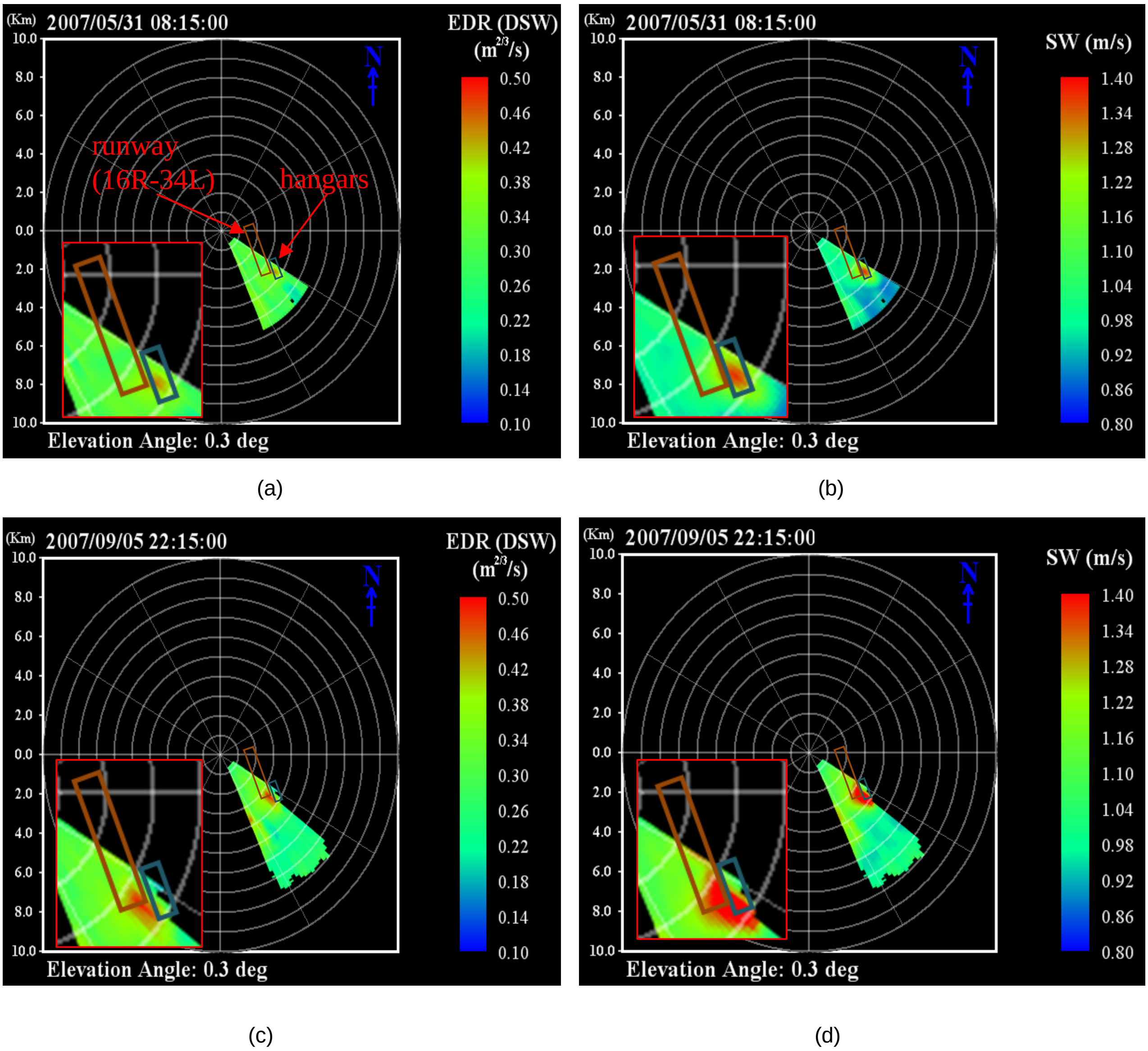

Figure 4 EDR maps (a) and (c), and spectrum width maps (b) and (d), for the two cases under study in the present paper. The insets show the zoom-in of the plots in the runway and hangar area.